


Article

The Fingerprints of Periodic Electric Fields on Line Shapes Emitted in Plasmas

Ibtissem Hannachi ^{1,2,†} and Roland Stamm ^{1,*,†} ¹ PIIM UMR 7345, Aix-Marseille University, CNRS, 13013 Marseille, France; ibtissam.hannachi@univ-batna.dz² LRPRIM, University Batna 1, Batna 05000, Algeria

* Correspondence: roland.stamm@univ-amu.fr

† These authors contributed equally to this work.

Abstract: Periodic electric fields are found in many kinds of plasmas and result from the presence of collective fields amplified by plasma instabilities, or they are created by external sources such as microwave generators or lasers. The spectral lines emitted by atoms or ions in a plasma exhibit a frequency profile characteristic of plasma conditions, such as the temperature and density of charged particles. The fingerprints of periodic electric fields appear clearly on the line shape for a large range of frequencies and magnitudes of the oscillating electric field. Satellite structures appear near to multiples of the oscillation frequency and redistribute the intensity of the line far from the line center. The modeling of the simultaneous effects of the plasma microfield and of a periodic electric field has been active since the seventies, but it remains difficult to be conducted accurately since the quantum emitter is submitted to several time-dependent electric fields, each with their own characteristic time. We describe here a numerical approach which couples a simulation of the motion of charged plasma particles with an integration of the emitter Schrödinger equation. Resulting hydrogen line shapes are presented for different plasmas and periodic fields encountered in laboratory and astrophysical plasmas.

Keywords: stark broadening; periodic electric fields; computer simulation



Citation: Hannachi, I.; Stamm, R. The Fingerprints of Periodic Electric Fields on Line Shapes Emitted in Plasmas. *Atoms* **2023**, *11*, 128. <https://doi.org/10.3390/atoms11100128>

Academic Editor: Frank B. Rosmej

Received: 21 August 2023

Revised: 22 September 2023

Accepted: 5 October 2023

Published: 8 October 2023



Copyright: © 2023 by the authors. Licensee MDPI, Basel, Switzerland. This article is an open access article distributed under the terms and conditions of the Creative Commons Attribution (CC BY) license (<https://creativecommons.org/licenses/by/4.0/>).

1. Introduction

Many different kinds of plasmas have their radiative properties affected by the presence of periodic electric fields. Such fields may be applied by an external source such as a microwave generator or a laser, or they can be created within the plasma by a collective motion of charged particles initiated by density or temperature gradients. Line shape changes due to oscillating electric fields have been studied since the beginning of quantum mechanics, with, e.g., Blokhintsev [1], who considered the spectrum of one Stark component in an electric field with a $\cos(\Omega t)$ time dependence. The Blokhintsev spectrum consists of satellites which are separated from the main line by multiples of the oscillation frequency Ω , and they have their intensity scaled with the square of the Bessel functions of integer order [1]. Interest was taken in performing the simultaneous diagnostic of plasma and longitudinal plasma oscillation parameters with the work of Baranger and Mozer [2] in 1961. In the following decades, many studies observed and analyzed the formation of structures generated by oscillating electric fields [3–5]. At the same time, many theoretical approaches have been proposed for the different kinds of plasmas studied (see the monographs Refs. [6–8] and the references therein). The problem with most of the line shape calculations is that they are based on numerous approximations since Stark broadening is a complex problem involving plasma and quantum physics. We study here only hydrogen atoms, for which approximations such as neglecting the Stark effect between states with a principal quantum number n other than those of the radiating transition, or the use of a dipole interaction, can be the source of inaccuracy on the line shape for dense plasma conditions [9]. For weakly coupled plasmas considered in the following, one often has to

retain ion dynamics together with the oscillating electric field for obtaining an accurate line shape. Here we achieve this goal with a computer simulation of the plasma particles coupled to a numerical integration of the Schrödinger equation. We show how the first Lyman and Balmer lines are modified in the presence of a periodic electric field with a magnitude of the order or larger than the plasma microfield.

2. Computer Simulation for the Plasma Particles

A common approach in plasma spectroscopy consists of using a static approximation for the ion perturbers and a binary impact approximation for the electrons [10]. The use of an impact operator for electron broadening is usually well justified for weakly coupled plasmas (plasma for which the mean kinetic energy is larger than the Coulomb potential energy). A simple validity criterion for this binary collision picture is that the decorrelation (memory loss) time t_0 of the emitter radiation (also called time of interest) is much larger than the electronic collision time $t_{ce} = r_0/v_e$, where r_0 is the typical interparticle distance defined by $r_0 = 0.62N_e^{-1/3}$, with N_e being the electron density, and v_e being the thermal electron velocity. A static approximation for the ions can be used if $t_0 \ll t_{ci}$, where $t_{ci} = r_0/v_i$, with v_i being the thermal ion velocity, thus ensuring that the interaction with the emitter is constant. It is well known today that this static approximation is rarely valid for weakly coupled plasmas, in particular for the first lines of the hydrogen series. Thus, one has to consider the time-dependent interaction of simultaneous strong collisions between the emitter and a large number of ions. Such conditions take place as the ionic strong collision radius, also called ionic Weisskopf radius $\rho_{wi} = \hbar n^2 / (m_e v_i)$, with m_e being the electron mass [6], which becomes larger than the typical interparticle distance r_0 . It can be verified that $\rho_{wi} > r_0$ for the lines and plasma conditions used in the following. Since no analytical approach can accurately account for the effect of multiple strong collisions on the emitter, we have used a computer simulation coupled to a numerical integration of the Schrödinger equation. Such simulations have become commonplace over the last decades thanks to the availability of convenient numerical means [11–13]. Following the reduced mass model [14], a basic simulation consists of placing the emitter at rest at the center of a cubic box and letting a few hundred fictitious perturbers with the reduced mass of the emitter–perturber pair move around the emitter. Perturber velocities are distributed according to a Maxwellian law, and for a neutral emitter, we assume that the perturbers move with straight line trajectories. We use periodic boundary conditions to ensure that the number of perturbers remains constant. A simple expression for the emitter–perturber interaction potential $V(t)$ is provided by a dipole approximation $V(t) = -\vec{D} \cdot \vec{E}(t)$, where \vec{D} is the emitter dipole, and $\vec{E}(t)$ is the electric field felt by the emitter. This approximation requires that the plasma particles stay far away from the emitter, a condition which is not always satisfied, e.g., in high-density plasmas. Several studies taking into account a full Coulomb interaction and considering perturbers penetrating the bound electron wave function have demonstrated how the line shapes can be modified in high-density plasmas [9,15,16]. Here we assume that we can use a dipole approximation, and we express the Debye screened electric field created by the i th ion by the expression:

$$\vec{E}_i = \left(\frac{e}{4\pi\epsilon_0} \right) \frac{\vec{r}_i}{r_i^3} \left(1 + \frac{r_i}{\lambda_D} \right) \exp\left(-\frac{r_i}{\lambda_D} \right), \quad (1)$$

where \vec{r}_i is the position of the i th ion, and the Debye length is defined by

$$\lambda_D = \sqrt{\epsilon_0 k_B T / (N_e e^2)} \quad (2)$$

where ϵ_0 is the permittivity of free space, k_B is the Boltzmann constant, T is the hydrogen plasma temperature, and e is the electron charge. The validity of such an independent quasiparticle model can be checked by using molecular dynamics simulations [17–19].

Significant differences with a quasiparticle model appear for strongly coupled plasma conditions. A molecular dynamics simulation would also allow to retain the effect of the oscillating electric field on the trajectory of the plasma particles. The study of this effect on the line shape is beyond the scope of this paper, but it would be of interest for the highest magnitudes of the oscillating field considered in the following calculations.

3. Line Shape Calculations

In the line shape calculations presented in the following, we simulate only the ions and retain the effect of the electrons using a collision operator ϕ_e . The oscillating electric field is assumed to have a single frequency Ω and a random phase φ . Such a simple model has been used since the beginning of the study of the effect of periodic fields on line shapes [2,20]. With the initial condition $U(0) = 1$, we solve numerically the emitter Schrödinger equation for the emitter evolution operator $U(t)$:

$$i\hbar \frac{dU(t)}{dt} = \left[H_0 + i\hbar\phi_e - \vec{D} \cdot \vec{E} - \vec{D} \cdot \vec{E}_W \cos(\Omega t + \varphi) \right] U(t), \quad (3)$$

where H_0 is the Hamiltonian of the unperturbed hydrogen atom, \vec{E} is the sum of the electric fields of the plasma ions at time t , and E_W is the magnitude of the oscillating electric field. The time-independent Hamiltonian $H_0 = p^2/2\mu - e^2/(4\pi\epsilon_0 r)$ is expressed here in the center of a mass system, with p being the relative momentum, r the distance between the proton and electron, and μ the reduced mass of the two particles. We use the Griem, Kolb, and Shen [21] electronic collision operator defined by:

$$\phi_e = C \frac{N_e}{v_e} \vec{D} \cdot \vec{D} \left[1 + \int_{y_{min}}^{\infty} \frac{e^{-y}}{y} dy \right], \quad (4)$$

where C is a constant, and $y_{min} = (\rho_{we}/\lambda_D)^2$ the square of the ratio of the electronic Weisskopf radius to the Debye length [21]. Different algorithms may be used for solving the Schrödinger equation, such as those using an implicit scheme [22].

The time step for the integration is chosen to be much smaller than the inverse of the fluctuation frequency $\omega_f = v_i/r_0$ and the inverse of the oscillation frequency. The integration is performed up to the order of the time of interest t_0 , and repeated for a set of histories, each one with different initial conditions. The knowledge of $U(t)$ provides the value of the dipole operator at time t :

$$\vec{D}(t) = U^\dagger(t) \vec{D} U(t). \quad (5)$$

After an average over a set of histories, it is possible to obtain the dipole autocorrelation function $C(t)$, a quantity showing how the dipole radiation is gradually decorrelated by the presence of different electric fields:

$$C(t) = \text{Tr} \left\{ \vec{D} \cdot \vec{D}(t) \rho \right\}_{av}, \quad (6)$$

where the brackets denote an average over a set of histories, and ρ is the density matrix, which will be assumed to be diagonal and time-independent in the following, as is customary for many line broadening calculations [6]. The line shape $I(\omega)$ is given by the real part of a Fourier transform:

$$I(\omega) = \frac{1}{\pi} \text{Re} \int_0^\infty C(t) e^{i\omega t} dt. \quad (7)$$

Other computer simulations of the line shape which allow for obtaining the same level of statistical noise with a reduced number of histories are often used today [23,24]. They use the Fourier transform of the time-dependent dipole (see Equation (5)) and calculate

the power spectrum. Here we stay with the calculation of $C(t)$ and use several thousand histories for limiting the statistical noise.

4. Results

4.1. Various Possible Calculations

The computer simulation described in Section 3 can be adapted to deal with various problems. The oscillating electric field magnitude E_w can be taken as constant among the different histories, or it may be sampled using a probability distribution function (PDF) expected in a non-equilibrium plasma. In the following, we use for some of the calculations a half-normal PDF, as predicted in strongly turbulent plasmas [25]. In all cases, we compare the magnitude E_w or its mean to the mean magnitude of the plasma microfield E_m , a quantity which can be calculated by our simulation, and is approximately equal to $3.4 E_0$ in a weakly coupled plasma [6], where E_0 is the electric field created by a proton at the mean interparticle distance r_0 . In most of the calculations presented, we use an oscillating frequency $\Omega = \omega_p$, with $\omega_p = \sqrt{N_e e^2 / m_e \epsilon_0}$ the electronic plasma frequency. For the conditions of Figures 1–3, $\omega_p = 1.78 \times 10^{13}$ rad/s, which is about one thousand time smaller than the angular frequency of the Lyman- α transition. Calling ω_0 the angular frequency of the radiative transition, it is easy to verify that for all the cases studied, $\omega_p \ll \omega_0$, with a difference of at least two orders of magnitude. As a result, for all the lines calculated, the resonance effects of the oscillating electric field are expected only with transitions between the Stark sublevels belonging to a level with the same principal quantum number. If a fixed direction of the oscillating field is assumed, we take the z axis along it, and the line shape becomes dependent on the angle θ between the line of sight and the z axis. The line shape can be expressed as:

$$I(\omega, \theta) = I_{\parallel}(\omega) \cos^2 \theta + I_{\perp}(\omega) \sin^2 \theta \quad (8)$$

where the intensities parallel and perpendicular to z can be expressed in terms of the σ and π components of the line shape [26]. As in the early models for the effect of Langmuir waves [2], the calculations carried out for this work assume that the oscillating electric field has a random direction, leaving the line shapes independent of the viewing angle θ . The line shapes presented in the following are plotted using a frequency ω measured from zero frequency located at the position of the unperturbed line. Only positive values of ω are shown since in our model (dipole interaction, no fine structure), the line shape is symmetric around the frequency $\omega = 0$. All the line shapes are presented in units of the plasma frequency, allowing for a comparison of the locations of satellites and multiples of the plasma frequency.

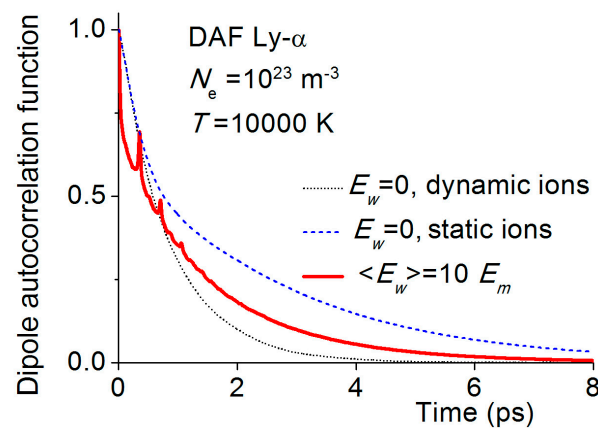


Figure 1. Ly- α dipole autocorrelation function (DAF) for static ions (dashed line) and dynamic ions (dotted line) without wave ($E_w = 0$), and for dynamic ions with a wave of mean magnitude $\langle E_w \rangle \geq 10 E_m$ (solid line). For the plasma conditions $N_e = 10^{23} \text{ m}^{-3}$ and $T = 10,000 \text{ K}$, $E_m = 2.7 \times 10^7 \text{ V/m}$.

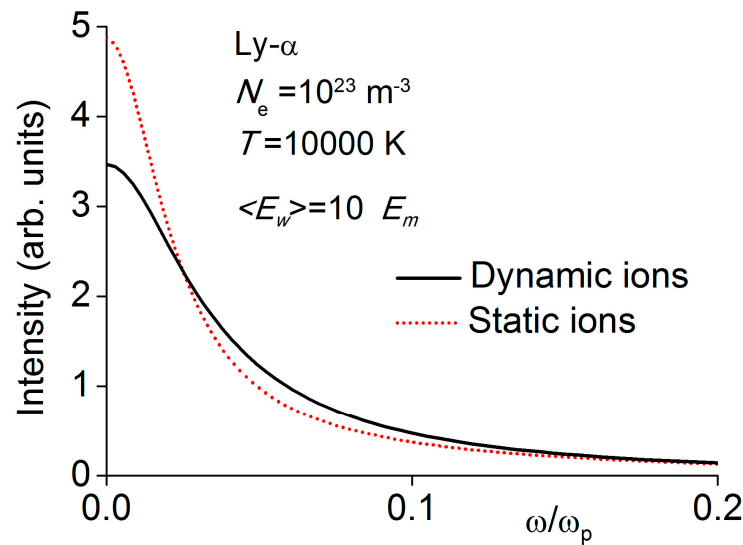


Figure 2. Central part of Ly- α line shapes in presence of a wave with a mean magnitude $\langle E_w \rangle \geq 10 E_m$. For the plasma conditions $N_e = 10^{23} \text{ m}^{-3}$ and $T = 10,000 \text{ K}$, $E_m = 2.7 \times 10^7 \text{ V/m}$ and $\omega_p = 1.78 \times 10^{13} \text{ rad/s}$.

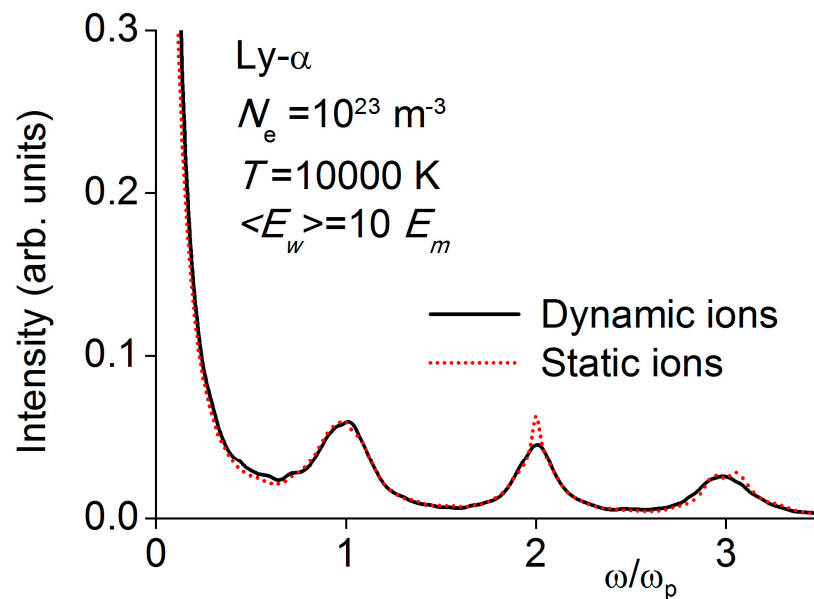


Figure 3. Wing of Lyman alpha line shapes with the conditions of Figure 2.

4.2. Lyman- α (Ly- α)

The $n = 2$ to $n = 1$ Lyman- α radiative transition is affected by ion dynamics for a large range of laboratory plasma conditions [27], and it is interesting to study the simultaneous effect of an oscillating electric field. In Figure 1, we plot the Ly- α dipole autocorrelation functions (DAFs) for a density $N_e = 10^{23} \text{ m}^{-3}$ and a temperature $T = 10,000 \text{ K}$. The DAF obtained for $E_w = 0$ is not affected by a periodic field but shows the difference between a calculation retaining ion dynamics (dotted line) and a static ion approximation (dashed line). The dynamic ions DAF appear to be more strongly decorrelated than the static ions DAF for intermediate and long times (here a long time is about 2 ps), suggesting that the central part of the line shape will be affected by ion dynamics. Note that the DAF indicates the value of the time of interest t_0 , which is also an estimate for choosing the upper integration time of the Schrödinger equation. The last DAF plotted is calculated for dynamic ions in the presence of an oscillating electric field with a mean magnitude $\langle E_w \rangle \geq 10 E_m$ (solid

line), obtained after a sampling over a Gaussian PDF. The DAF is strongly decorrelated for short times, and structures appear at multiples of $t_p = 2\pi/\omega_p$.

For times larger than about 1 ps, the decorrelation becomes slower than for the dynamic ions DAF without a wave. Line shapes obtained by the Fourier transform of the dynamic and static DAF and in the presence of a field $\langle E_w \rangle \geq 10 E_m$ are shown in Figure 2 for the central part, and in Figure 3 for the line wing. In Figure 2, one observes an increase of about 50% of the linewidth when ion dynamics are retained (solid line), an increase which is, however, much smaller than for the line calculated without the oscillating field, for which the dynamic ions line is three time broader than the static ions line. Here, the dynamics of the oscillating field prevails over that of the ionic field and transfers a part of the central intensity to satellites located at multiples of the plasma frequency. The first three satellites are shown in Figure 3 and show the residual effect of ion dynamics, with a smearing out of the second satellite peak, and the filling of a small dip appearing on the third satellite. In summary for this line, one fingerprint of the oscillating electric field is the appearance of the satellites, around which dynamic effects can still be observed near to the location of the satellite. A second fingerprint is a reduction in Stark broadening, which is in particular visible in the central part of the line, a phenomenon which was already pointed out as a possible way for improving laser gain [28,29].

4.3. Balmer- α ($H\alpha$)

We plot in Figure 4 the central part of the $H\alpha$ line for a density $N_e = 10^{22} \text{ m}^{-3}$ and a temperature $T = 10,000 \text{ K}$ in the presence of an oscillating electric field with a mean magnitude $\langle E_w \rangle = 5 E_m$. The halfwidth of the profile calculated by retaining ion dynamics is about 25% larger than for the static ion case. This difference is much smaller than for a calculation in the absence of an oscillating electric field, where it is of a factor of about two.

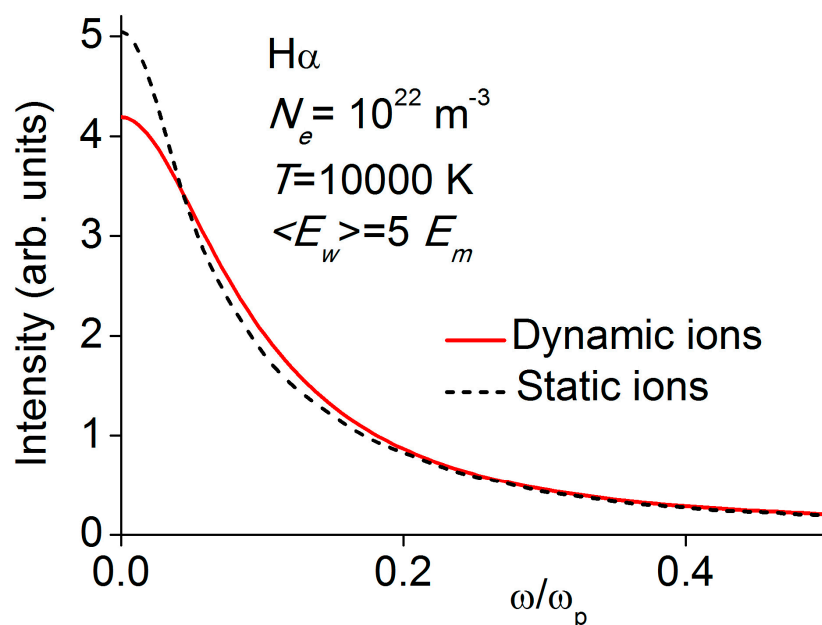


Figure 4. Balmer alpha line shapes in presence of a wave with a mean magnitude $\langle E_w \rangle \geq 5 E_m$: central part of the line. For the plasma conditions $N_e = 10^{22} \text{ m}^{-3}$ and $T = 10,000 \text{ K}$, $E_m = 5.9 \times 10^6 \text{ V/m}$, and $\omega_p = 5.64 \times 10^{12} \text{ rad/s}$.

Everything happens as if there is a competition between the effect of ion dynamics and the effect of the periodic field. In the presence of this periodic field, the transfer of intensity occurs from the central region of the line toward several satellites located in the wing of the line where the ion dynamics effect is reduced. This is shown in Figure 5, where the static and dynamic ions satellites are almost identical. The difference seen between the

two calculations for the third and subsequent satellites is a measure of the statistical noise, which increases as one moves towards the line wing [24].

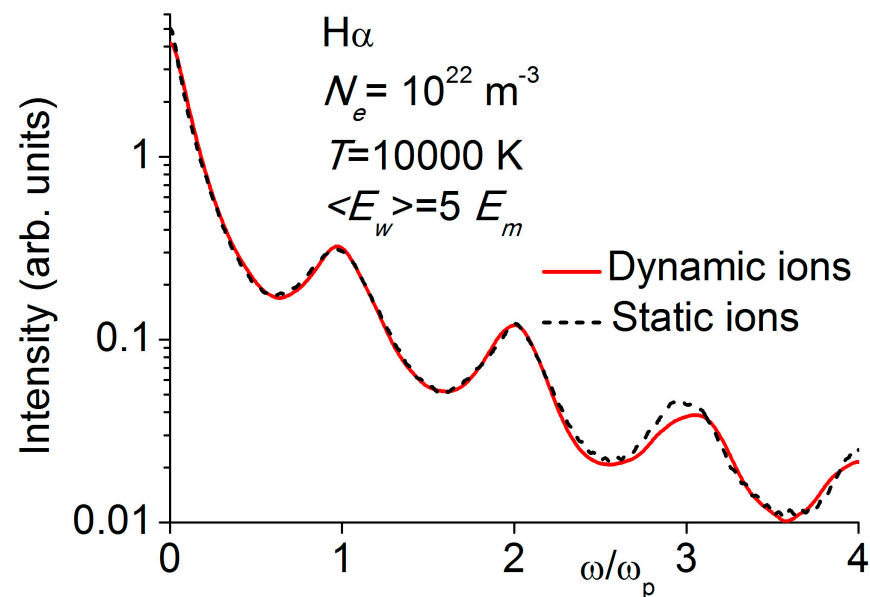


Figure 5. Satellites on the Balmer alpha line shapes in presence of a wave with a mean magnitude $\langle E_w \rangle \geq 5 E_m$.

4.4. Lyman- β ($Ly-\beta$)

We plot in Figure 6 the Lyman- β line shape for the same density and temperature as in Figure 5, for a mean magnitude of the oscillating field $\langle E_w \rangle \geq 3 E_m$, and three different values of the oscillation frequency $\Omega = 1, 2$ and $4 \omega_p$. The Stark profile without an oscillating electric field (solid line) is modified when any of the oscillation frequencies are applied, and satellites appear at multiples of the oscillation frequency. The most important changes are seen for $\Omega = \omega_p$, with a central intensity divided by a factor of two, and a first satellite with an intensity equal to two-thirds of the new central intensity of the line (dashed line). The changes in the central part of the line are reduced as the frequency is increased, and similarly, the intensity and the number of satellites are also reduced. A possible explanation of this behavior may be found in resonance effects between the oscillation frequency and the splitting of the Stark substates. The average Stark splitting is of the order of the central peak width (solid line), which is about one half of the plasma frequency. A resonance between the plasma frequency and the energy difference between Stark substates favors non-adiabatic interactions, which induce radiationless transitions to a different substate. A quantum mechanical evolution of the emitter retains the contribution of such non-adiabatic effects to the line formation. For the conditions of Figure 6, increasing the oscillation frequency reduces the possibility of such resonance effects, and thus decreases the effects of the periodic field.

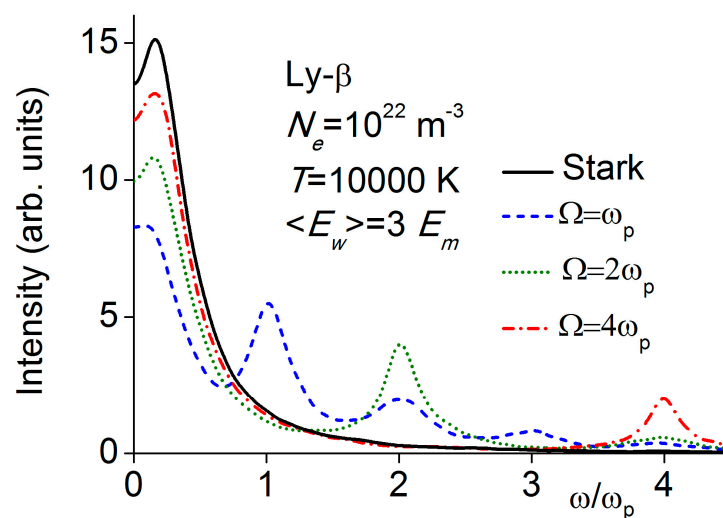


Figure 6. Lyman beta line shapes in presence of a wave with a mean magnitude $\langle E_w \rangle \geq 3 E_m$, and three different values of the oscillation frequency.

4.5. Balmer-β (Hβ)

In Figure 7, we show the effect of an oscillating electric field at frequency ω_p , with a mean magnitude $\langle E_w \rangle \geq 1$ and $3 E_m$, for a density $N_e = 10^{21} \text{ m}^{-3}$ and a temperature $T = 10,000 \text{ K}$. In a similar way to the Ly-β line in Figure 6, the average Stark splitting is about one half of the plasma frequency, suggesting a significant effect of the periodic field on the line shape.

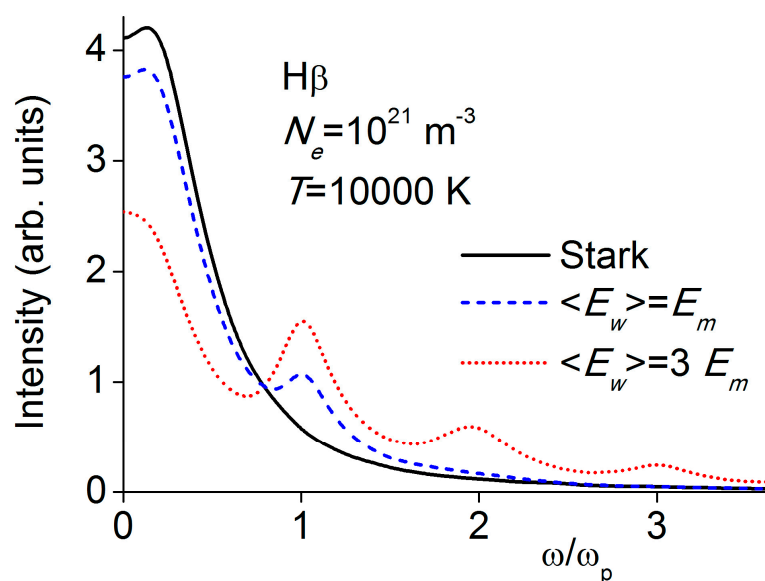


Figure 7. Balmer beta (Hβ) line shapes in presence of a wave with a mean magnitude $\langle E_w \rangle$ equal to 1 and $3 E_m$. For the plasma conditions $N_e = 10^{21} \text{ m}^{-3}$ and $T = 10,000 \text{ K}$, $E_m = 1.3 \times 10^6 \text{ V/m}$, and $\omega_p = 1.78 \times 10^{12} \text{ rad/s}$.

For $\langle E_w \rangle \geq E_m$, the intensity of the central part of the line without a periodic electric field (solid line) is reduced by about 10%, and a satellite with an intensity of about 40% of the new central intensity (dashed line) can be seen. A much stronger distortion of the line is observed for $\langle E_w \rangle \geq 3 E_m$, with a first satellite having an intensity of about 60% of the central intensity, and two other satellites visible at two and three times the plasma frequency. For this case, one observes a significant transfer of the intensity of the central part of the line to several satellites, resulting also in a narrowing by 12% of the line

measured at half width at half maximum. Such line distortions have been observed on H β for similar plasma conditions in early experiments [3] in a turbulent plasma. We plan to apply our simulation to revisit such early observations, but also to analyze more recent spectra obtained in dense plasmas.

5. Conclusions

A computer simulation model for Stark line shapes in the presence of a periodic electric field with a magnitude of the order or larger than the mean plasma microfield has been described and applied for the calculation of the first Lyman and Balmer lines of hydrogen. The complex simultaneous effects of ion dynamics, electron broadening, and the oscillating electric field is retained on the quantum emitter by a numerical solution of the Schrödinger equation. As the wave magnitude increases, a fraction of the central intensity of the line is transferred to satellites located at multiples of the oscillation field frequency. Our model may be used in future developments for non-hydrogenic emitters in dense plasmas, and it can be upgraded by adding the effect of a magnetic field. We also plan to use the fingerprints of periodic electric fields to develop a simultaneous accurate diagnostic of plasma and the oscillating electric field parameters.

Author Contributions: Formal analysis, I.H.; Writing—review & editing, R.S. All authors have read and agreed to the published version of the manuscript.

Funding: This research received no external funding.

Data Availability Statement: The data that support the findings of this study are available from the corresponding author upon reasonable request.

Acknowledgments: One of us (I.H.) would like to thank the PIIM laboratory for supporting several stays in Marseille.

Conflicts of Interest: The authors declare no conflict of interest.

References

1. Blokhintsev, D. Theory of the Stark effect in a time-dependent field. *Phys. Z. Sow. Union* **1933**, *4*, 501–515.
2. Baranger, M.; Mozer, B. Light as a plasma probe. *Phys. Rev.* **1961**, *123*, 25–28.
3. Gallagher, C.; Levine, M. Observation of H β satellites in the presence of turbulent electric fields. *Phys. Rev. Lett.* **1971**, *27*, 1693–1696. [[CrossRef](#)]
4. Rutgers, W.; de Kluiver, Z. The dynamic Stark-effect in a turbulent hydrogen plasma. *Z. Naturforsch.* **1974**, *29*, 42–44.
5. Nee, T.; Griem, H. Measurement of hydrogen n- α -line Stark profiles in a turbulent plasma. *Phys. Rev. A* **1976**, *14*, 1853–1868.
6. Griem, H. *Spectral Line Broadening by Plasmas*; Academic Press: New York, NY, USA, 1974; ISBN 0-12-302850-7.
7. Lisitsa, V. *Atoms in Plasmas*; Springer: Berlin, Germany, 1994; ISBN 3-540-57580-4.
8. Oks, E. *Plasma Spectroscopy*; Springer: Berlin, Germany, 1995; ISBN 3-540-54100-4.
9. Sobczuk, F.; Dzierzega, K.; Stambulchik, E. Plasma Stark effect of He II Paschen- α : Resolution of the disagreement between experiment and theory. *Phys. Rev. E* **2022**, *106*, L023202.
10. Griem, H. *Principles of Plasma Spectroscopy*; Cambridge University Press: Cambridge, UK, 1997; ISBN 0-521-45504-9.
11. Stamm, R.; Voslamber, D. On the role of ion dynamics in the Stark broadening of hydrogen lines. *J. Quant. Spectrosc. Radiat. Transf.* **1979**, *22*, 599–609.
12. Stambulchik, E.; Maron, Y. Plasma line broadening and computer simulations: A mini-review. *High Energy Density Phys.* **2010**, *6*, 9–14.
13. Ferri, S.; Calisti, A.; Mossé, C.; Rosato, J.; Talin, B.; Alexiou, S.; Gigosos, M.; Gonzales, M.; Gonzales-Herrero, D.; Lara, N.; et al. Ion dynamics effect on Stark-broadened line shapes: A cross-comparison of various models. *Atoms* **2014**, *2*, 299–318.
14. Seidel, J.; Stamm, R. Effects of radiator motion on plasma-broadened hydrogen Lyman- β . *J. Quant. Spectrosc. Radiat. Transf.* **1982**, *27*, 499–503.
15. Gomez, T.; Nagayama, T.; Cho, P.; Zammit, M.; Fontes, C.; Kilcrease, D.; Bray, I.; Hubeny, I.; Dunlap, B.; Montgomery, M.; et al. All-order full-Coulomb quantum spectral line shape calculations. *Phys. Rev. Lett.* **2021**, *127*, 235001.
16. Stambulchik, E.; Iglesias, C. Full radiator-perturber interaction in computer simulations of hydrogenic spectral line broadening by plasmas. *Phys. Rev. E* **2022**, *105*, 055210.
17. Stamm, R.; Talin, B.; Pollock, E.; Iglesias, C. Ion-dynamic effects on the line shapes of hydrogenic emitters in plasmas. *Phys. Rev. A* **1986**, *34*, 4144–4152.

18. Stambulchik, E.; Maron, Y. A study of ion-dynamics and correlation effects for spectral line broadening in plasma: K-shell lines. *J. Quant. Spectrosc. Radiat. Transf.* **2006**, *99*, 730–749.
19. Gigosos, M.; Gonzalez-Herrero, D.; Lara, N.; Florido, R.; Calisti, A.; Ferri, S.; Talin, B. Classical molecular dynamics simulations of hydrogen plasmas and development of an analytical statistical model for computational validity assessment. *Phys. Rev. E* **2018**, *98*, 033307.
20. Oks, E.; Sholin, G. Stark profiles of hydrogen spectral lines in a plasma with Langmuir turbulence. *Sov. Phys. JETP* **1975**, *41*, 482–488.
21. Griem, H.; Kolb, A.; Shen, K. Stark broadening of hydrogen lines in a plasma. *Phys. Rev.* **1959**, *116*, 4–16.
22. Koonin, S. *Computational Physics*; Addison Wesley: Redwood City, CA, USA, 1986; ISBN 0-201-12279-0.
23. Stambulchik, E.; Alexiou, S.; Griem, H.; Kepple, P. Stark broadening of high principal quantum number hydrogen Balmer lines in low-density laboratory plasmas. *Phys. Rev. E* **2007**, *75*, 016401.
24. Rosato, J.; Marandet, Y.; Stamm, R. Quantifying the statistical noise in computer simulations of Stark broadening. *J. Quant. Spectrosc. Radiat. Transf.* **2020**, *240*, 107002.
25. Robinson, P.; Newman, D. Strong Langmuir turbulence generated by electron beams: Electric-field distributions and electron scattering. *Phys. Fluids B* **1990**, *2*, 3120–3133.
26. Peyrusse, O. Spectral line-shape calculations for multielectron ions in hot plasmas submitted to a strong oscillating electric field. *Phys. Rev. A* **2009**, *79*, 013411.
27. Stambulchik, E.; Demura, A. Dynamic Stark broadening of Lyman- α . *J. Phys. B At. Mol. Opt. Phys.* **2016**, *49*, 035701. [[CrossRef](#)]
28. Oks, E. Enhancement of X-ray lasers by narrowing of the lasing spectral line due to a dressing by optical laser radiation. *J. Phys. B At. Mol. Opt. Phys.* **2000**, *33*, L801–L805.
29. Alexiou, S. X-ray laser line narrowing: New developments. *J. Quant. Spectrosc. Radiat. Transf.* **2001**, *71*, 139–146.

Disclaimer/Publisher's Note: The statements, opinions and data contained in all publications are solely those of the individual author(s) and contributor(s) and not of MDPI and/or the editor(s). MDPI and/or the editor(s) disclaim responsibility for any injury to people or property resulting from any ideas, methods, instructions or products referred to in the content.